EARTH SURFACE PROCESSES AND LANDFORMS
Earth Surf. Process. Landforms **35**, 803–816 (2010)

Published online 28 January 2010 in Wiley InterScience
(www.interscience.wiley.com) DOI: 10.1002/esp.1976

Coevolution of hydrology and topography on a basalt landscape in the Oregon Cascade Range, USA

A. Jefferson,[1]* G.E. Grant,[2†] S.L. Lewis[3] and S.T. Lancaster[3]
[1] Department of Geography and Earth Sciences, University of North Carolina at Charlotte, 9201 University City Boulevard, Charlotte, NC 28223, USA
[2] USDA Forest Service, Pacific Northwest Research Station, 3200 SW Jefferson Way, Corvallis, OR 97331, USA
[3] Department of Geosciences, Oregon State University, 104 Wilkinson Hall, Corvallis, OR 97331, USA

Received 17 July 2009; Revised 11 November 2009; Accepted 17 November 2009

*Correspondence to: A. Jefferson, Department of Geography and Earth Sciences, University of North Carolina at Charlotte, 9201 University City Boulevard, Charlotte, NC 28223, USA. E mail: ajefferson@uncc.edu
†The contribution of G.E. Grant to this article was prepared as part of his official duties as a United States Federal Government employee.

ESPL
Earth Surface Processes and Landforms

ABSTRACT: Young basalt terrains offer an exceptional opportunity to study landscape and hydrologic evolution through time, since the age of the landscape itself can be determined by dating lava flows. These constructional terrains are also highly permeable, allowing one to examine timescales and process of geomorphic evolution as they relate to the partitioning of hydrologic flowpaths between surface and sub-surface flow. The western slopes of the Cascade Range in Oregon, USA are composed of a thick sequence of lava flows ranging from Holocene to Oligocene in age, and the landscape receives abundant precipitation of between 2000 and 3500 mm per year. On Holocene and late Pleistocene lava landscapes, groundwater systems transmit most of the recharge to large springs (≥0·85 $m^3 s^{-1}$) with very steady hydrographs. In watersheds >1 million years old, springs are absent, and well-developed drainage networks fed by shallow subsurface stormflow produce flashy hydrographs. Drainage density slowly increases with time in this basalt landscape, requiring a million years to double in density. Progressive hillslope steepening and fluvial incision also occur on this timescale. Springs and groundwater-fed streams transport little sediment and hence are largely ineffective in incising river valleys, so fluvial landscape dissection appears to occur only after springs are replaced by shallow subsurface stormflow as the dominant streamflow generation mechanism. It is proposed that landscape evolution in basalt terrains is constrained by the time required for permeability to be reduced sufficiently for surface flow to replace groundwater flow.

KEYWORDS: landscape evolution; flowpaths; groundwater; basalt; Cascade Range

Introduction

Understanding the processes driving landscape evolution is of fundamental interest to geomorphologists. Landscape evolution, as reflected in the degree of drainage network development, influences many other hydrologic and geomorphic processes, including streamflow response to precipitation, groundwater residence times, and sediment delivery processes. In turn, these processes are first-order controls on the sensitivity of landscapes to land use and climate change.

In many parts of the world, fluvial incision and concomitant hillslope and mass wasting processes are primary drivers of landscape evolution (Whipple and Tucker, 1999). Peak discharges with 1–5 year recurrence intervals do much of the geomorphic work in a fluvial landscape (Wolman and Miller, 1960), and highly variable precipitation producing flashy hydrographs results in more efficient erosion than steady rainfall and discharge (Tucker and Bras, 2000; Wu *et al.*, 2006). Fluvial incision is controlled by the streamflow generation process (Dunne, 1980), which is itself a function of the climate, topography, soils, and bedrock (Horton, 1933; Hewlett and Hibbert, 1967; Anderson and Burt, 1978; Beven and Kirkby, 1978; Onda *et al.*, 2006; Soulsby *et al.*, 2006).

Numerous field and modeling studies have investigated the effects of various combinations of climate, soils, and bedrock on runoff generation and landscape evolution (Ijjasz-Vasquez *et al.*, 1992; Onda, 1992; Tucker and Bras, 1998; Hattanji and Onda, 2004; Huang and Niemann, 2006). Few of these studies have focused on landscapes with high permeability, where rapid infiltration of water into large subsurface aquifers precludes surface runoff and results in groundwater discharge that tends to be very steady over time. Such permeable landscapes are found in regions underlain by unconsolidated sediments, limestone, fractured rock, and young basalt lava flows (Dohrenwend *et al.*, 1987; White, 2002). The purpose of this study is to investigate the co-evolution of streamflow generation mechanisms, hydrograph characteristics, drainage network development, and landscape dissection on a young

basalt landscape in the Oregon Cascade Range. We seek to understand how the high initial permeability of such a landscape affects the rate and sequence of hydrologic and geomorphic processes, and may constrain the timescales necessary for drainage evolution. Although focused on a specific locale, we expect this work to highlight and inform our knowledge of the poorly understood linkage between landscape evolution and the partitioning of precipitation between surface and shallow subsurface runoff contributing to flood hydrographs and deeper subsurface recharge contributing to baseflow.

Of all landscapes, those constructed by basalt lava flows have some of the highest permeabilities (10^{-5} to 10^{-10} cm^2) (Freeze and Cherry, 1979), and the additional advantage of being independently datable, using radiocarbon, $^{40}Ar/^{39}Ar$, K/Ar and other dating methods. Basalt landscapes are also widespread across Earth's climatic regions. Basalt landscapes thus provide the opportunity to rigorously constrain timescales of drainage network development on initially permeable substrates. Hydraulic conductivity within and between basalt flows can vary by orders of magnitude (Welhan and Reed, 1997), because of very high porosity and permeability associated with vesicles, cooling fractures, and rubble zones at flow tops and bottoms. Individual basalt lava flows are 1–20 m thick, so a vertical section of 100 m or more encompasses many near-horizontal high permeability zones at each of the flow boundaries, and young basalt landscapes comprising these layered flows therefore have a high overall permeability (Davis, 1969; Kilburn, 2000). Many basalt landscapes are characterized by major aquifers, sinking streams, and large springs (Meinzer, 1927; Stearns, 1942; Rose *et al.*, 1996; Kiernan *et al.*, 2003).

The effects of young basalt lavas on surface and subsurface drainage patterns have long been recognized (Stearns, 1942), and a relationship between permeability, weathering, and drainage development was postulated by Cotton (1942). Baker (1988) proposed that drainage evolution on volcanoes proceeds as a function of climate, relief, rock type, and time. Thus, if three factors are held constant, the effect of one variable, such as time, can be studied by assembling a sequence of landscapes spanning a range of ages. Chronosequences of drainage development on basalts have been observed in varying climates throughout the world, including Hawaii (Kochel and Piper, 1986; Baker and Gulick, 1987), southwestern USA (Wells *et al.*, 1985; Dohrenwend *et al.*, 1987; Eppes and Harrison, 1999), Iceland (Gislason *et al.*, 1996), and Jordan (Allison *et al.*, 2000). These chronosequences show a progression from recently emplaced lava with no surface drainage to deeply dissected landscapes with well developed stream networks. These previous studies suggest a general trend of increasing fluvial incision and drainage density over timescales of 0·1–5 million years. Climate appears to play a role in defining this rate, but clear causal linkages and climatic controls are not well established.

Various conceptual models have been formulated to explain the evolutionary sequence, with the models invoking phenomena such as a substantial stream power threshold for incision (Bishop *et al.*, 1985), groundwater seepage erosion (Kochel and Piper, 1986; Baker and Gulick, 1987; Kochel and Baker, 1990), mantling with fine-grained eolian material (Dohrenwend *et al.*, 1987; Eppes and Harrison, 1999), subsurface clay accumulation during soil development (Lohse and Dietrich, 2005), and major landslides combined with waterfall erosion (Lamb *et al.*, 2007). Distinguishing among these various mechanisms is problematic, however, in part because of difficulty in making process-level observations of driving mechanisms. Here we use stream hydrology as an additional source of information to illuminate the driving processes.

In this work, we examined the features and timescales of drainage development in the Oregon Cascade Range, where basalts have been erupted for over 35 million years (Sherrod and Smith, 2000). Undissected Holocene basalts with major aquifers are juxtaposed against adjacent deeply dissected Pliocene-upper Eocene basalts along the western slopes of the Cascade Range (Ingebritsen *et al.*, 1992; Jefferson *et al.*, 2006; Luo and Stepinski, 2008). Hydrologic and geomorphic differences between the Holocene and the Pliocene and older landscapes have been recognized (Grant, 1997; Tague and Grant, 2004), but the timescales of and controls on drainage network development in this environment are unexplored.

Our goal is to understand the coevolution of hydrology and geomorphology in the Oregon Cascade Range and to do so in a way that might be applicable to other initially permeable landscapes around the world. We combine data from stream hydrographs, USGS topographic maps, and digital elevation models with observations of fluvial and spring geomorphology in nine watersheds with dated rock units from 1400 years old to 7 million years old (Ma).

Study Area

Our study area lies on the western slopes of the central Oregon Cascade Range (Figure 1), a volcanic arc formed by the subduction of the Juan de Fuca plate under the North American Plate. The Oregon Cascade Range is commonly divided into two subprovinces: High Cascades and Western Cascades. The High Cascades lie mostly within a graben where extensive Quaternary and Pliocene volcanism has been associated with nearly 3 km of rift-related subsidence in the last 5 million years (Conrey *et al.*, 2002). This region has produced mostly basalt and basaltic andesite lavas from shield volcanoes and cinder cones, but also has interspersed composite volcanoes of more diverse composition (Sherrod and Smith, 2000). The crest of the range lies 1500–2000 m above sea level, with the high peaks exceeding 3000 m. The Western Cascades represents the Miocene-upper Eocene arc, with dacitic tuffs, andesite lava flows, and lesser basaltic and rhyolitic volcanic rocks (Conrey *et al.*, 2002); peak elevations reach 1800 m.

The Cascade Range has been subjected to three Pleistocene glaciations, each of which formed an ice cap over the Cascade crest with outlet glaciers carving U-shaped valleys down eastward- and westward-draining rivers (Scott, 1977). Glaciation also occurred in the higher elevations of the Western Cascades, as evidenced by cirques and U-shaped valleys (Swanson and Jones, 2002). The last glacial advance of the Pleistocene occurred between 11,000 and 12,500 years before present (yr BP) (Scott and Gardner, 1990). Two minor glacial advances occurred in the past 8000 years. At present, glaciers are restricted to the flanks of the composite volcanoes. There is evidence for sub-glacial volcanic activity in palagonites exposed at North Sister (Schmidt *et al.*, 2002) and isolated tuya forms (Conrey *et al.*, 2002). Most pre-Holocene High Cascades volcanoes show extensive glacial erosion and large swaths of Pleistocene lavas are blanketed by till.

The High Cascades are the major source of summer streamflow to western Oregon (Tague and Grant, 2004; Jefferson *et al.*, 2007), owing to the steady discharge of groundwater stored in the young basalts (Jefferson *et al.*, 2006, 2008). Western Cascades watersheds have flashy event hydrographs resulting from shallow subsurface stormflow (i.e. runoff-dominated streams) (Rothacher, 1965; Tague and Grant,

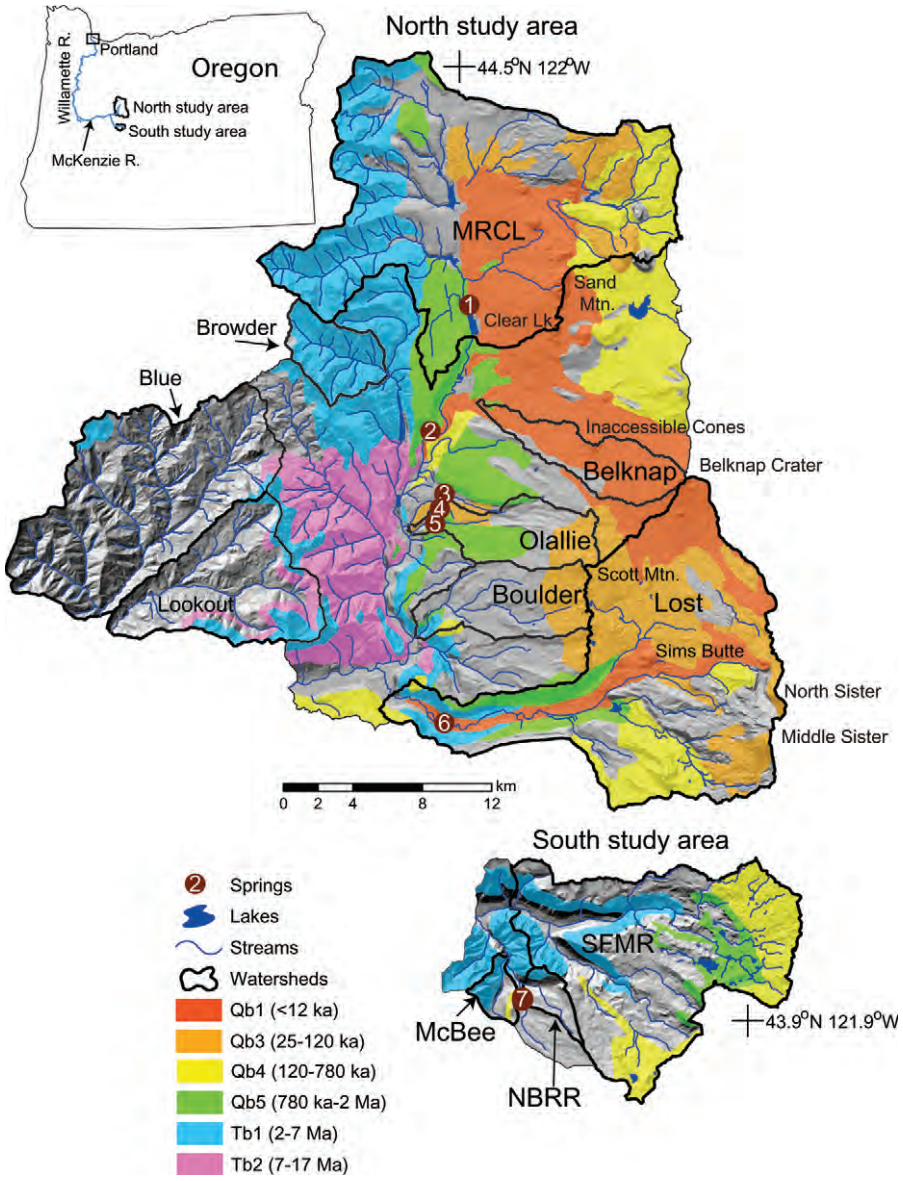

Figure 1. Map of study areas, showing geology and topography. Study watersheds are outlined and labeled, and volcanic peaks referred to in the text are labeled. Basalt and basaltic andesite units are as mapped by Sherrod and Smith (2000). Large springs are labeled from north to south: [1] Great Spring; [2] Tamolitch Spring; [3] Sweetwater Spring; [4] Olallie North Spring; [5] Olallie South Spring; [6] Lost Spring; and [7] Roaring Spring. Stream network shown as mapped on 1:24,000 USGS maps. This figure is available in colour online at www.interscience.wiley.com/journal/espl

2004). The Quaternary basalts of the High Cascades are characterized by high permeability (~10^{-5} to 10^{-7} cm^2) for the upper several hundred meters (Manga, 1997; Saar and Manga, 2004; Jefferson *et al.*, 2006). In the Western Cascades, equally high permeability is exhibited only in the 1–3 m deep soil mantle (Dyrness, 1969; Harr, 1977).

Western Cascades watersheds have been studied extensively, largely because of work associated with the H.J. Andrews Experimental Forest (http://andrewsforest.oregonstate.edu/), which encompasses the watershed of Lookout Creek (USGS gage # 14161500). Soils are generally loamy with poorly developed profiles, and have extremely high infiltration capacities; no overland flow occurs except on artificially compacted soils (Dyrness, 1969). Exposed bedrock is sometimes present in upper reaches of streams, but most reaches are alluvial step-pool streams. Channel and valley morphology is strongly influenced by low frequency, high-magnitude floods and debris flows (Grant *et al.*, 1990; Grant and Swanson, 1995). Shallow landslides and debris flows following heavy precipitation events are major sources of sediment to streams and do much of the geomorphic work (Swanson and Fredriksen, 1982).

In the Cascade Range, more than 70% of annual precipitation falls between November and March. Seasonal snowpacks form above 1200 m, with transient snowpacks and rain occuring below 1200 m. There is a strong orographic effect, with ~2 m of precipitation at lower elevations and up to 3·8 m on peaks along the Cascade Range crest (Taylor and Hannan, 1999). Distributed precipitation climatology data are available through the parameter–elevation regressions on independent slopes model climate mapping system (Daly *et al.*, 2002). Vegetation varies with rock age and elevation. Forests are dominated by Douglas fir (*Pseudotsuga menziesii*), western hemlock (*Tsuga heterophylla*), and western redcedar (*Thuja plicata*) at lower elevations, and have noble fir (*Abies procera*), Pacific silver fir (*Abies amabilis*), Douglas fir, and western hemlock at higher elevations. Vine maple (*Acer circinatum*) is also common on Holocene and Pleistocene lava flows.

Table I. Characteristics of the study watersheds

Watershed	Weighted age based on best available data (ka)*	Watershed area (km^2)	Elevation range (m)	Mean elevation (m)	Percentage basalt and basaltic andesite**	Percentage glacial deposit**	Annual precipitation (m)***	WY04 mean unit discharge ($m^3\ s^{-1}\ km^{-2}$)
High Cascade								
Belknap	17	27·1	901–2086	1412	89	11	2·16	–
Olallie Creek	84	29·7	609–1858	1224	65	33	2·12	0·140
Boulder Creek	180	32·7	533–1859	1227	37	63	2·12	0·009
Lost Creek	182	197	520–3075	1603	79	6	2·49	0·030
North Branch Roaring River (NBRR)	230	6·84	1155–1671	1413	12	88	1·88	0·106
South Fork McKenzie River (SFMR)	541	136	805–2064	1452	49	51	1·96	0·028
McKenzie River at the outlet of Clear Lake (MRCL)	576	238	918–2051	1215	77	13	2·20	0·049
McBee Creek	1068	6·38	962–1733	1246	59	41	1·87	0·049
Browder Creek	2242	20·1	839–1651	1239	98	0	2·70	0·050^
Western Cascade								
Lookout Creek	8000	62·4	434–1628	986	28	0	2·22	0·051
Blue River below Tidbits Creek	15534	117	432–1628	974	4·2	0	2·22	–^^

* Best available data includes mapping by Sherrod and Smith (2000), Sherrod *et al.* (2004), Schmidt and Grunder (2009) $^{40}Ar/^{39}Ar$ dates published in this study, and ^{14}C dates calibrated in this study.
** Based on Sherrod and Smith (2000).
*** Derived from parameter-elevation regressions on independent slopes model (PRISM) precipitation estimates for the 1971–2000 climate normal period (Daly *et al.*, 2002).
^ Discharge data for Browder Creek is based on USGS gage #14158790 (Smith River above Smith River Reservoir)
^^ USGS gage #14161100 was discontinued on 30 September 2003.

Within the McKenzie River watershed, we selected nine study watersheds that capture the full exposed range of High Cascades rock ages (Figure 1). Three study watersheds are tributary to the South Fork of the McKenzie River, and these will be referred to as the south study area. Six of the watersheds lie within the area upstream of McKenzie Bridge (USGS stream gage #14159000); these will be referred to as the north study area. The McKenzie Bridge watershed covers an area of 901 km^2, 68% of which is basalt or basaltic andesite, and has an elevation range of 435 to 3075 m.

The nine High Cascades study watersheds range in size from 6 to 238 km^2 (Table I). The three watersheds in the south study area are McBee Creek, North Branch of the Roaring River (NBRR), and the South Fork of the McKenzie River above Frissell Crossing (SFMR). SFMR has two prominent glacial troughs. In the north study area, the study watersheds are Belknap, Boulder Creek, Browder Creek, Lost Creek, McKenzie River at the outlet of Clear Lake, and Olallie Creek. The Lost Creek watershed includes the western slopes of two composite volcanoes, North and Middle Sister, and a prominent glacial trough.

For purposes of comparison between the High Cascades and Western Cascades, data from two typical Western Cascades watersheds are also presented. These two watersheds, which also lie within the McKenzie River watershed, are Lookout Creek (USGS gage # 14161500) and Blue River below Tidbits Creek (USGS gage # 14161100). The bedrock geology of the Western Cascades watersheds is more silicic than that of the High Cascades watersheds, reflecting the typical lithological differences between the two subprovinces of the Oregon Cascade Range. Examining these watersheds allows us to evaluate whether the High Cascades landscape evolves toward hydrology and landscape form that is similar to the Western Cascades.

Methods

Mapped and dated rock units were used to constrain timescales of drainage development and to calculate weighted average ages for each study watershed. Sherrod and Smith (2000) mapped volcanic rocks of the Oregon Cascade Range and divided the Eocene through present into ten age classes, six of which are present in the study area as basalts and basaltic andesites (Figure 1). Maps by Sherrod *et al.* (2004) and Schmidt and Grunder (2009) provide more detail, particularly of late Quaternary lava flows, but only cover parts of the study area. Weighted ages for each watershed were calculated by multiplying the fractional area of each rock unit by a corresponding age. Ages were determined using the best available data (Sherrod and Smith, 2000; Sherrod *et al.*, 2004; Schmidt and Grunder, 2009). Age assignments for rock units mapped by Sherrod *et al.* (2004) and Schmidt and Grunder (2009) were based on ages assigned in those publications. Rock units of Sherrod and Smith (2000) were assigned to the lower limit of their age class, because these assignments provided the closest match to $^{40}Ar/^{39}Ar$ and radiocarbon dates on the same units within the study watersheds.

Mapped and previously dated rock units were supplemented with three $^{40}Ar/^{39}Ar$ ages. We collected samples in the vicinity of three springs for $^{40}Ar/^{39}Ar$ dating of rock age, in order to constrain the range of ages of rocks hosting major aquifers. Major and trace element chemistry data for the samples are published by Jefferson *et al.* (2006), and spring locations are shown in Figure 1. At Roaring Spring, a basaltic andesite sample (AJ-04-5) was collected from the spring orifice. A basalt sample (AJ-04-3) was obtained from an outcrop 10 m from Olallie North Spring. Olallie South spring emerges from beneath a talus slope, so a basalt sample (AJ-05-5) was collected from an outcrop above the talus slope as

a best estimate of the groundwater-bearing strata. Whole rock samples were analyzed using a MAP 215-50 rare gas mass spectrometer at the Noble Gas Laboratory, College of Oceanographic and Atmospheric Sciences, Oregon State University. Incremental heating in a double-vacuum resistance furnace released argon gas over five or six steps following the methods of Duncan and Hogan (1994). Ages were calculated using ArArCalc version 2·2 software (Koppers, 2002), and age plateaus were defined as three or more contiguous heating steps that yielded ages within error of each other. Errors cited on $^{40}Ar/^{39}Ar$ ages are all 2σ (95% confidence level). Data tables with complete Ar analyses, irradiation constants, and age calculations for each sample are archived at http://www.earthref.org. Radiocarbon (^{14}C) ages from Sherrod *et al.* (2004) were calibrated using OxCal v.4.0.5 (Bronk Ramsey, 1995, 2001) and the IntCal04 atmospheric calibration curve (Reimer *et al.*, 2004). The calibrated calendar age used for estimating watershed age is the weighted mean of the 1σ sigma distribution.

To quantify discharge patterns from study watersheds, we established stream gages in previously ungaged watersheds. In July 2003, water level recorders were installed on Boulder Creek, Lost Creek, McBee Creek, North Branch Roaring River, Olallie Creek, and South Fork McKenzie River. Stage–discharge relationships were developed using standard methods (Carter and Davidian, 1968) and daily discharges were calculated for the period of 13 July 2003 to 10 December 2004. There is a USGS gage at McKenzie River at the outlet of Clear Lake (USGS gage # 14158500). No gage was installed in Browder Creek because there is a USGS gage (#14158790) on Smith River, to which Browder Creek drains. The Browder Creek watershed comprises 48% of the Smith River watershed, and the geology of both watersheds is predominantly 2–7 Ma basalts (Sherrod and Smith, 2000). No gage was installed in the Belknap watershed because there is no stream. In order to calculate the stormflow and baseflow contributions to the stream hydrographs, were performed graphical hydrograph separations were performed for water year 2004 (1 October 2003 to 30 September 2004) using the sliding interval of Pettyjohn and Henning (1979) and Sloto and Crouse (1996).

One measure of the level of drainage development in a landscape is drainage density, which is defined as the length of stream in the watershed divided by watershed area (km km^{-2}). To calculate drainage density, we digitized stream networks from 'blue lines' on 1:24,000 USGS topographic maps. This 'blue line' stream network was compared to a valley detection algorithm of Luo and Stepinski (2008), which bases its delineation on the topographic curvature measured in the direction of the tangent to contour at a given point. Luo and Stepinski (2008) used this algorithm to show dissection density contrasts between the High and Western Cascades in Oregon, and found that it matched the blue line network better than other automated stream delineation algorithms. Eleven channel heads were located in the field using handheld GPS, for comparison to blue line and algorithm-based drainage networks. The channel heads were randomly selected, based on rock type and age class units of Sherrod and Smith (2000) and first-order blue lines. Drainage densities were calculated using both blue lines and the valley-detection algorithm for each study watershed and each rock type and age class of Sherrod and Smith (2000).

To further explore the degree of landscape development through time, we examined relationships between local slope and contributing area for the study watersheds following the precedents of Flint (1974), Montgomery and Dietrich (1989), Tarboton *et al.* (1992), and Stock and Dietrich (2003) among others. Such slope–area relationships allow comparison of the topographic signature of hillslope, debris flow, and fluvial processes within a watershed. Contributing areas and slopes for each DEM pixel in the watershed were computed with a D-infinite algorithm (Tarboton, 1997) on a 10 m DEM derived from 1:24,000 USGS topographic maps. Results were binned into 100-pixel groups sorted by contributing area. Average slopes for contributing areas <1 ha were also calculated. All statistical regressions were fitted using JMP, Version 7 (SAS Institute Inc., Cary, NC).

Results

Chronology

The nine High Cascades study watersheds have weighted average ages ranging from 17 thousand years ago (ka) to 2242 ka (2·2 Ma). The youngest basalts in the study area are those from Belknap Crater (1310 ± 110 to 1500 ± 180 yr BP; Sherrod *et al.*, 2004). These basalts are located in the Belknap and Lost watersheds. The oldest basalts in the study area are 7–17 Ma; these rocks outcrop in the Western Cascades Blue and Lookout watersheds and in a small area near the outlet of the Boulder watershed. Weighted ages and watershed characteristics for the nine study watersheds are reported in Table I.

Three new $^{40}Ar/^{39}Ar$ dates constrain ages for the lava flows from which several large springs emerge. Olallie North Spring discharges from a Scott Mountain basalt lava (Jefferson *et al.*, 2006), and an $^{40}Ar/^{39}Ar$ date of 35,000 ± 25,000 years was determined. A date younger than 12,500 yr BP is unlikely since all Scott Mountain lavas are covered with glacial till at higher elevations. Another large spring, Sweetwater Spring, also emerges from Scott Mountain lava and a similar age is presumed. The sample from the cliff above Olallie South Spring yielded an age of 535,000 ± 63,000 years. In the south study area, Roaring Spring emerges from basaltic andesite with an $^{40}Ar/^{39}Ar$ age of 684,000 ± 40,000 years.

Fluvial hydrology and morphology

Striking contrasts exist among the hydrographs of the study watersheds (Figure 2). During water year 2004, five watersheds had annual peak flows more than 10 times greater than the minimum flow during the same period. In the other three watersheds, annual peak flows were 250 times greater than the minimum flow. Field reconnaissance, USGS topographic maps, and 0·6 m resolution aerial photographs demonstrate that Belknap watershed has no surface drainage, so there are no discharge data to report. The five watersheds with damped hydrograph variability had baseflow >94% of total annual flow, but in the three flashy watersheds baseflow contributed <85% of the annual flow. Damped hydrographs are typical of spring-fed streams in the Oregon Cascade Range, and four of the five damped hydrograph streams in this study are known to be sourced in large springs. Flashy hydrographs are characteristic of regional streams fed by shallow subsurface stormflow (Manga, 1999; Tague and Grant, 2004; Jefferson *et al.*, 2008), and only one of the three flashy streams in this study has a mapped spring in its watershed. The mapped spring in the Boulder Creek watershed is a small seep, as determined by observation.

Watershed age is a moderate predictor of the percentage baseflow (Figure 3), suggesting that watersheds may evolve from having a damped hydrograph almost entirely consisting of groundwater-fed baseflow to a flashy hydrograph with lower baseflows. Comparison of the study watersheds with the

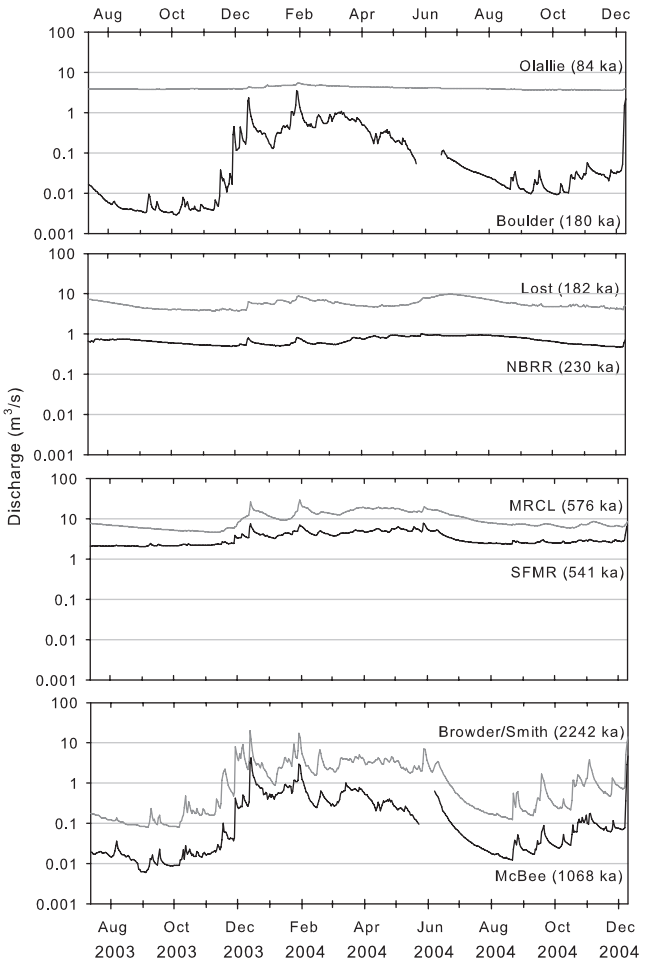

Figure 2. Hydrographs of streams in High Cascades watersheds from 13 July 2003 to 10 December 2004. Tick marks represent the first day of each month. MRCL is gaged by the USGS (# 14158500). Browder watershed composes 48% of the Smith River watershed area, and Smith River is gaged by the USGS (#14158790). Data are reported as measured at the Smith River gage. Data gaps for Boulder and McBee result from equipment failure.

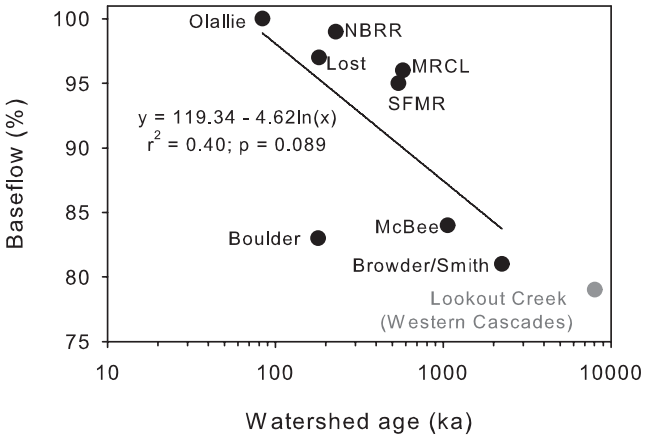

Figure 3. Percentage of baseflow composing hydrographs in High Cascade watersheds in water year 2004 (1 October 2003 to 30 September 2004) versus watershed age. Hydrographs were separated using the sliding interval graphical methods of Pettyjohn and Henning (1979) and Sloto and Crouse (1996). Data from Lookout Creek in the Western Cascades are plotted for comparison, data from Blue River are not available for water year 2004.

Western Cascades 8000 ka Lookout watershed suggests that percentage baseflow will continue to decline over time at a rate similar to that observed in the High Cascades.

Boulder watershed (180 ka) differs from the pattern of stable hydrographs in young watersheds and flashy hydrographs in older watersheds. The unit discharge of Boulder Creek is substantially lower than other streams in the study area, and previous work on probable groundwater flowpaths suggests that some precipitation falling on Boulder watershed may go to recharge aquifers that feed the springs in Olallie watershed (Jefferson *et al.*, 2006). We suggest the flashy hydrograph of Boulder Creek is a result of shallow subsurface flow on the older, early Pleistocene–Pliocene portions of the watershed and the absence of bedrock groundwater discharge from younger portions of the landscape, due to that deeper water crossing the topographic drainage divide.

There are seven large springs (≥0·85 $m^3\ s^{-1}$) in the study area, and details of their hydrogeology are given by Jefferson *et al.* (2006). These large springs discharge from basalts ranging in age from 1310 ± 110 to 1500 ± 180 yr BP (Sherrod *et al.*, 2004) at Tamolitch Spring to 684,000 ± 40,000 yr BP at Roaring Spring. Discharge from the six large springs in the north study area was previously reported by Jefferson *et al.* (2006). On a unit area basis, large spring discharge is 0·067 $m^3\ s^{-1}\ km^{-2}$ on basalts and basaltic andesites <12 ka, declines to 0·026 $m^3\ s^{-1}\ km^{-2}$ on basalts and basaltic andesites between 25 and 780 ka, and is zero on older units. Large and small springs are identified on 1:24,000 USGS topographic maps. The density of springs drops from 0·07 per km^2 on Quaternary basalts to zero on Pliocene–Miocene basalts. Within Quaternary units there is no relationship between basalt age and spring density. These results suggest that the number and discharge of springs declines over time, and that there may be an upper bound on the age of rock that can host a large spring.

All of the large springs in the study area have morphologies that appear to be controlled by the constructional morphology of lava flows. Great Spring emerges into a ~12 m wide, 7 m deep pool along the lateral contact between two Sand Mountain lava flows (2830 ± 320 to 3140 ± 380 yr BP; Sherrod *et al.*, 2004). Water seeps out through multiple small orifices in the younger lava close to the pool surface, and the pool level fluctuates by <0·5 m seasonally. The spring drains to a 100 m channel entering Clear Lake. This channel is positioned in a small gap between the two lava flows. Local relief above the pool is ~5 m and exhibits the constructional morphology of aa lava. Tamolitch Spring emerges in the bed of McKenzie River at the base of an 18 m waterfall. With natural river discharges, the waterfall is dry except during snowmelt-runoff periods (April–June), because the entire discharge of the McKenzie River sinks into Belknap lava (1310 ± 110 to 1500 ± 180 yr BP; Sherrod *et al.*, 2004) and emerges 1·5 km further downstream at the spring at the base of the waterfall (Stearns, 1929). Groundwater emerges from fissures ~3 m above the spring pool and falls into the ~10 m deep pool. Since 1963, a hydroelectric project has diverted the McKenzie River around the losing reach and spring, and water emerging from the spring now seeps out below the pool level. The main Olallie North Spring cascades out of Scott Mountain lava and down a steep slope for 5 m, before joining Olallie Creek with water from secondary springs. The morphology of Olallie South Spring is obscured by large (≥1·5 m) talus blocks fallen from a cliff face to the south. The largest spring, Lost Spring emerges from Sims Butte basalt (7·6–20 ka; Sherrod *et al.*, 2004), 2·5 km upstream of the flow toe. The spring emerges over a broad area of >100,000 m^2 in a series of quiet shallow pools. Water levels in the pools vary <1 m annually. Surface flow appears and disappears several times before forming a

single-thread channel. Most pools are <1 m deep with <2 m local relief above the pool level. This topography appears to result from the constructional morphology of the lava flow. A similar morphology is observed at Sweetwater Spring, which emerges from Scott Mountain lava. Roaring Spring discharges from a horizontal fracture >100 m long at the top of a ~8 m cliff face.

There is no correlation between spring morphology and the age of the basalt from which the spring issues. Only Tamolitch Spring exhibits theater-headed valley morphology, and at that site there is some evidence for plunge pool erosion from the ephemeral waterfall, possibly a result of paleo-floods. Further, the applicability of a theater shape as diagnostic of seepage erosion in bedrock has been cast into serious doubt by the work of Lamb and others (2006; 2007; 2008). Other features that have been used to identify groundwater seepage erosion include overhanging alcoves, large rock debris in the pool, and evidence of sediment transport in the downstream channel (Dunne, 1990). None of the springs in the study area have these features. Seepage weathering has been inferred to occur where salt precipitation or freeze–thaw cycles occur at spring orifices, but no salt precipitation has been observed, and the springs flow at constant 4·5–6·3°C temperatures (Jefferson *et al.*, 2006), precluding freeze–thaw cycling. Thus, there is no evidence for seepage weathering or erosion at springs in the study area.

Downstream of the springs, spring-fed streams display morphologies contrasting with runoff-dominated streams. The channel downstream of Olallie North Spring (1·7 $m^3 s^{-1}$; Jefferson *et al.*, 2006) lies in a steep-sided valley that appears to result from a gap between lava flows rather than fluvial erosion. The channel occupies the entire valley bottom, which is <5 m wide near the spring and 18 m wide, 800 m downstream. The nearby channel below Olallie South Spring (2·3 $m^3 s^{-1}$; Jefferson *et al.*, 2006) is <3 m wide, conveys channel-filling discharge for most of the year, and lacks evidence for overbank flow or incision of a valley larger than the modern channel. No sediment transport in spring-fed channels was visually observed during field work over the full range of annual flows. Large wood in the channels shows no evidence of transport, and is moss-covered a few centimeters above the water surface. These observations are consistent with those made in spring-fed channels on the east side of the Oregon Cascade Range (Whiting and Stamm, 1995; Whiting and Moog, 2001). In contrast, runoff-dominated Boulder Creek has step-pool morphology and large wood jams, and has been observed to flow overbank and transport bed material. Based on morphology and lack of evidence for sediment transport, spring-fed streams do not seem to be effective geomorphic agents of valley incision, possibly because they lack large floods, transported sediment to act as fluvial tools, and/or sufficient time for bedrock incision.

Drainage development

Despite the observations that water discharged from springs does not appear to be eroding channels, drainage density increases with time for basalts in the north study area (Figure 4a). USGS blue line and valley-detection algorithm-derived networks both show an increase in drainage density with time, with the algorithm delineating greater stream lengths and higher drainage densities for every age unit. The majority of the study area is covered with basalt lava, so we are unable to compare drainage densities on basalts with those on rock units of similar age but differing lithologies.

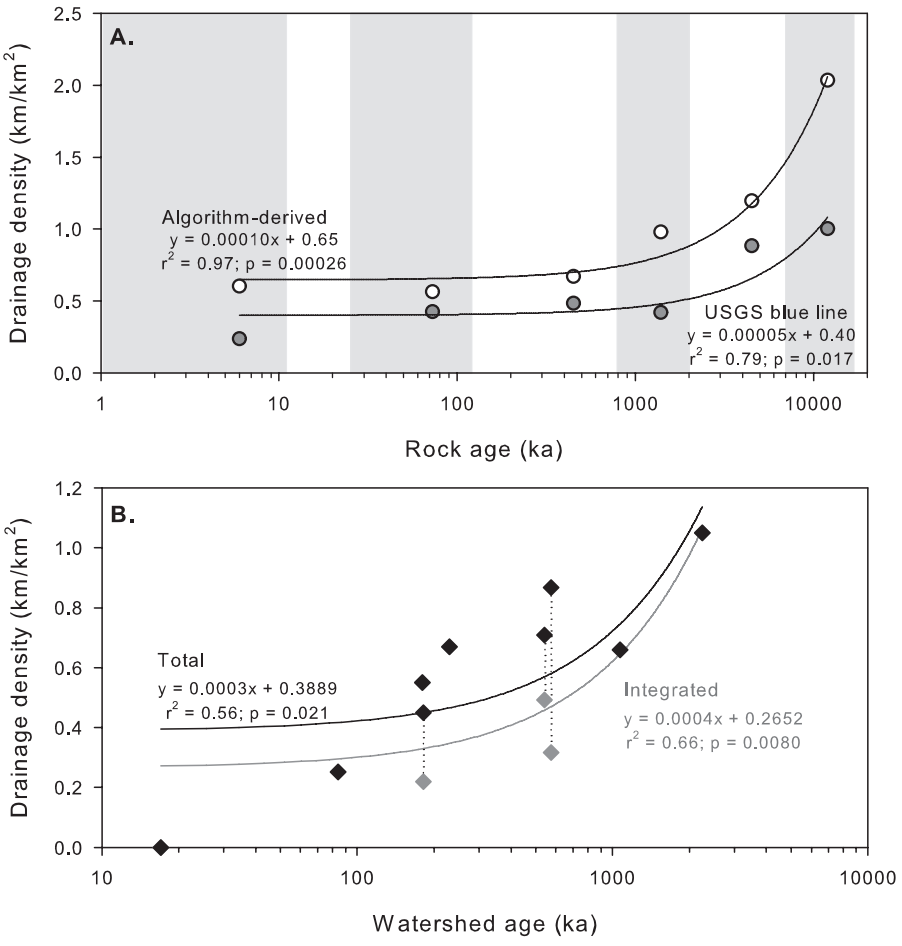

Figure 4. Drainage density versus rock unit and watershed age. (A) Drainage density of basalts and basaltic andesites in the north study area. Stream lengths were measured from digitized 1:24,000 topographic maps (gray circles) and obtained from the valley detection algorithm published by Luo and Stepinski (2008) (white circles). Shaded bars represent the range of ages for map units of Sherrod and Smith (2000), and circles represent the median age of each unit. The regression lines were fitted through the median ages. (B) Black diamonds represent the total drainage density of each study watershed. Gray diamonds represent integrated drainage density of watersheds where integrated drainage density is lower than total drainage density. Integrated drainage density is defined as the length of stream connected to the watershed outlet, divided by watershed area. Lengths of streams that drain to closed basin lakes or wetlands are not counted in the integrated drainage density calculation. Dashed lines show the relationship between total drainage density and integrated drainage density for specific watersheds.

Locations of 11 field-observed channel heads on Pleistocene and Pliocene–Miocene basalts were compared with the upstream termini of the blue line and algorithm-derived networks. The distance between the blue line termini and field-observed channel heads ranges from 30 to 1100 m, with eight channel heads <250 m from USGS mapped locations. The location of one channel head was >1000 m from the mapped location, in a low-relief wet-meadow area. The distance between algorithm-derived valley termini and field-observed channel heads ranges from 110 to 8600 m, with five channel heads more than 1000 m from their algorithm-derived locations. There was no trend with age for rocks older than 25 ka in the distance between field-observed and USGS mapped or algorithm-derived channel heads, although the sample sizes were very small. Based on this metric, we conclude that the USGS blue line network is a better indicator of fluvial channels in the study area than the valley detection algorithm of Luo and Stepinski (2008). However, we are unable to find any evidence for two of the USGS mapped first order streams on Holocene lavas. This suggests that the blue line network could substantially overestimate the extent of stream channels developed on the youngest basalts, and that true drainage density might be lower than that calculated. Additionally, the drainage density of the oldest Quaternary basalt map unit (Qb5, Figure 1) is limited by the rocks' exposure primarily along ridgelines where contributing areas are low.

Despite these uncertainties, the overall trend of increasing drainage density with basalt age is demonstrated by both the USGS blue line network and the valley detection algorithm. These results show that there is a continuum of drainage development from Holocene to Pliocene basalts in the study area. Based on a linear regression, drainage density increases at a rate of ~0·1 km km^{-2} Ma^{-1} (Figure 4a), but this regression allows drainage density to be >0 when the landscape is constructed. The blue line data is equally well fitted by a logarithmic regression, and the fit is improved by assuming zero drainage density on 1 ka rocks. The resulting regression is $y = 0{\cdot}093 \ln(x) + 0{\cdot}65$, where y is drainage density (km km^{-2}), x is rock age (ka), and the least squares fit (r^2) is 0·79 ($P = 0{\cdot}018$). This result suggests that drainage density increases relatively quickly on young basalts, and the rate of increase slows on older rocks.

The increase in drainage density with rock age is supported by a general increase in drainage density with age for the nine High Cascades study watersheds (Figure 4b). The highest drainage densities in the High Cascades are comparable with drainage densities in the Western Cascades Lookout (0·73 km km^{-2}) and Blue (1·1 km km^{-2}) watersheds. Drainage density values calculated for watersheds exhibit more scatter than do those calculated for single rock types, possibly reflecting the influence of glacial till on drainage development. Till has a drainage density of 0·56 km km^{-2} in the north study area, and most of the stream length in the Boulder and NBRR watersheds is on till.

In the Lost, MRCL, and SFMR watersheds, substantial stream lengths are not connected to the trunk stream and instead drain to closed basins. These closed basins are the result of lava-dammed lakes and deranged drainage of glacial origin. We define an integrated drainage density as the length of stream connected to the watershed outlet, divided by watershed area. Lengths of streams that drain to closed basin lakes or wetlands are not counted in the integrated drainage density calculation. Integrated drainage densities for Lost, MRCL, and SFMR are 31 to 63% lower than the standard measurement of drainage density. Integrated drainage density is also a significantly better predictor of hydrograph behavior than the standard drainage density (Figure 5). Integrated drainage density may covary with hydrograph characteristics because it expresses both the lengths and topology of surface water and groundwater routing. Water may move by shallow subsurface stormflow to a stream and contribute to a peak flow in a closed basin, but that peak flow is subsequently filtered and damped by transmission through the groundwater system and ultimately discharges as baseflow in a stream connected to the watershed outlet. Only water that moves by overland or shallow subsurface stormflow to a connected stream contributes to event flow at the watershed outlet, and integrated drainage density provides a measure of the network where such transmission is possible.

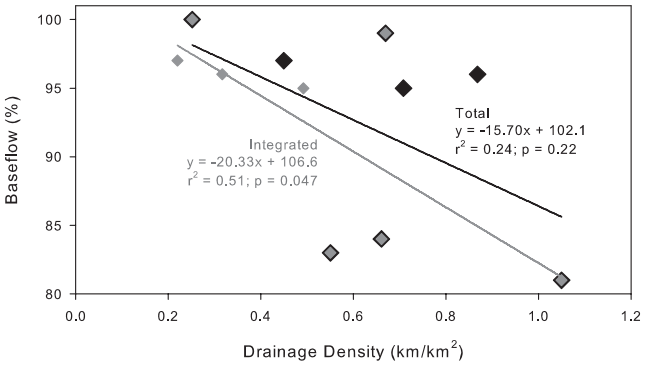

Figure 5. Drainage density versus percentage baseflow. Large black diamonds represent the total drainage density of each study watershed, and small gray diamonds represent integrated drainage density. Points in which gray and black diamonds are superimposed represent watersheds where total drainage density and integrated drainage density are the same. Integrated drainage density is defined as the length of stream connected to the watershed outlet, divided by watershed area.

Landscape dissection

The relationship between contributing area and local slope was examined for the nine study watersheds, in order to understand the timescales and processes of landscape dissection (Figure 6). Local slopes and upslope contributing areas were calculated for each DEM pixel based on its elevation relative to neighboring cells, as fully described in the methods section.

Belknap (17 ka), Olallie (84 ka), Boulder (180 ka), and Browder (2242 ka) watersheds are of similar size and elevation range, but diverge in their degree of landscape dissection. Each watershed is tributary to the upper McKenzie River, and lacks cirques, U-shaped valleys, and other features of glacial erosion. Belknap, Boulder Creek, and Olallie Creek watersheds are all on the flanks of shield volcanoes, which typically have constructional slopes of 0·07 to 0·14 (Walker, 2000). Areas distal from the volcano may be influenced by preexisting topography. Minor parts of the watersheds are occupied by cinder cones, which have constructional slopes averaging 0·4 and footprints averaging 0·33 km^2, based on Holocene cinder cones in the study area. The initial topographic conditions of Browder Creek watershed are more difficult to infer, but the style of volcanism in this segment of the Cascade Range arc has been similar for >5 million years (Conrey *et al.*, 2002), suggesting that the basalts likely originated from a shield volcano. Base level lowering through trunk stream incision has occurred throughout the past 5 million years, so there is on-going transient response in all watersheds.

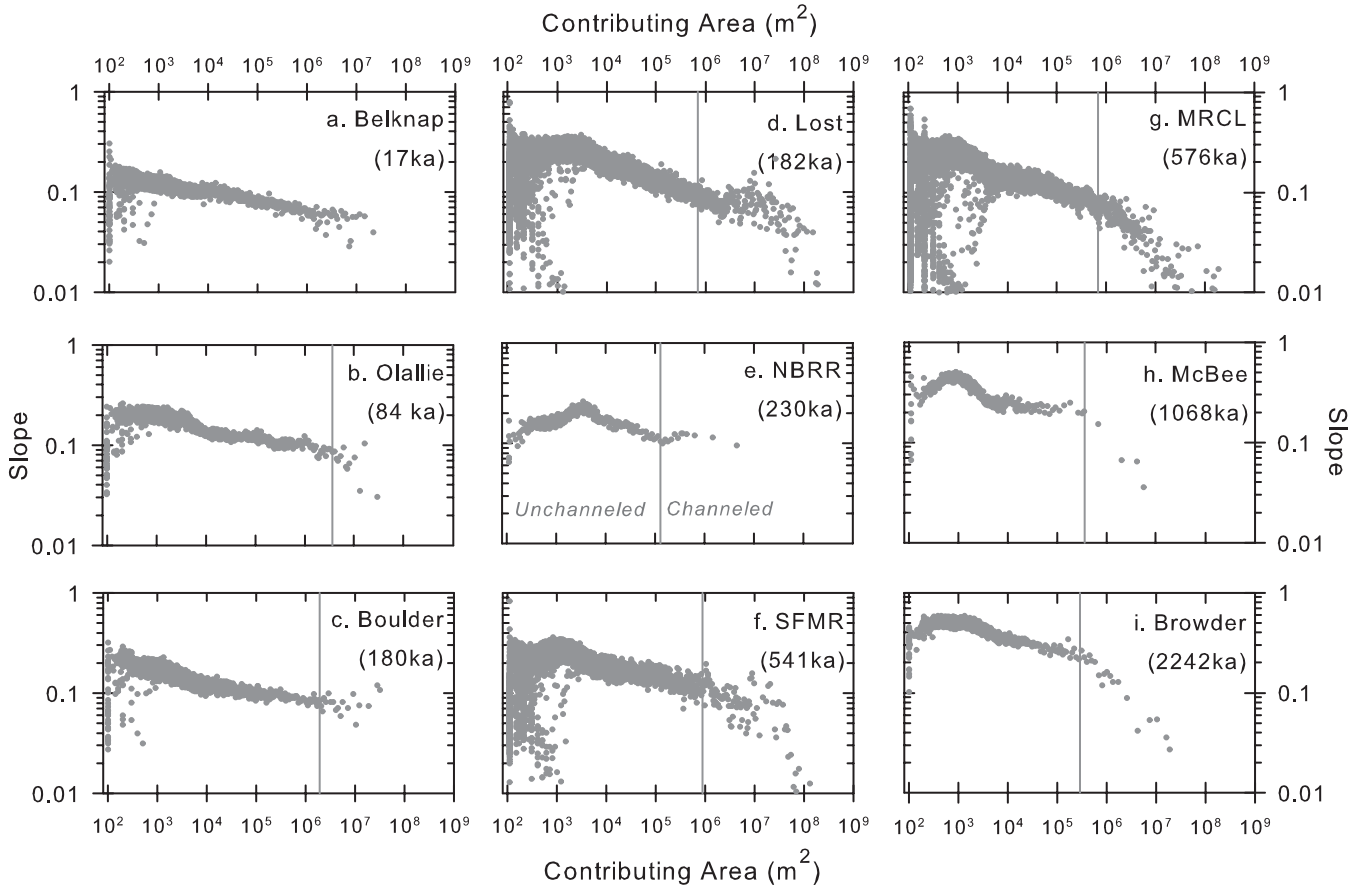

Figure 6. Slope–area relationships for High Cascades study watersheds. The vertical bar represents the average contributing area of channel heads in the watershed, with points to the left of the bar representing unchanneled areas and points to the right of the bar representing the stream network. There are no channels in the Belknap watershed.

The Belknap watershed (17 ka) lacks surface drainage, and has a land surface which consists predominantly of <5000 year old lavas from Belknap Crater and the Inaccessible Cones (88% of area). Field observations and aerial photographs show primary lava flow structures (e.g. pressure ridges, swales) on Belknap Crater lavas and provide no evidence for fluvial, glacial, or landslide erosion. Based on these observations, the Belknap slope–area relationship (Figure 6a) is interpreted to represent the constructional morphology of shield volcanoes, which typically have their steepest slopes near the summit. There is no break in slope at high contributing areas because there are no debris flow-dominated or fluvial channels present on the landscape.

Browder watershed (2242 ka) encompasses a third order stream, and the longitudinal profile for Browder Creek has a generally concave up shape with an average gradient of 4%. Channel heads in the watershed indicated by blue line termini on 1:24,000 topographic maps have an average contributing area of $2{\cdot}9 \times 10^5$ m^2. Somewhat above that value, the slope-area relationship shows a distinct inflection at a contributing area of 5×10^5 m^2 and slope of ~0·2 (Figure 6i). This inflection is inferred to represent the transition from debris flow channels to fluvial channels (Montgomery and Foufoula-Georgiou, 1993; Tucker and Bras, 1998). The slope at the inflection point is similar to field-observed debris flow–fluvial transitions in the Oregon Coast Range and Marin County, California (Montgomery and Foufoula-Georgiou, 1993), although it is higher than the ~0·03 to 0·1 reported by Stock and Dietrich (2003). Steep hillslopes in the watershed are scarred by debris flow tracks, with channels scoured to bedrock, and surrounding trees obliterated by the mass movement. These tracks are very similar to those observed in the Oregon Coast Range and elsewhere (Stock and Dietrich, 2003). The slope–area relationship for Browder Creek corroborates field observations of the importance of debris flows as a geomorphic process in older watersheds of the Oregon Cascade Range. Debris flows cannot initiate on such low slopes as those of constructional shield volcanoes, so some degree of landscape dissection by fluvial or glacial processes is a prerequisite for the initiation of debris-flow channels.

Adjacent Olallie (84 ka) and Boulder (180 ka) watersheds differ from each other in their source of streamflow, hydrograph characteristics, and drainage density (Table I). Olallie watershed has channels beginning at two large springs, and a concave stream profile with an average gradient of 7%. Boulder Creek watershed (180 ka) has a drainage density of 0·55 km km^{-2}, and the streams do not begin at large springs. Upslope of the channel heads, the slope–area relationships for the two watersheds are very similar, and there are no pronounced inflections in the slope–area trends for either the Olallie or Boulder watersheds (Figure 6b, 6c). The average contributing area of the Olallie springs is $3{\cdot}6 \times 10^6$ m^2 and there is considerable scatter in the slopes at greater contributing areas. For Boulder, slopes steepen slightly at areas $>1{\cdot}9 \times 10^6$ m^2, the average channel initiation point. The longitudinal profile of Boulder Creek has a distinct slope change in its lower reaches, representing an early transient response to continual base level lowering by the McKenzie River. Such a response may be possible in Boulder watershed with its flashy hydrograph, but not in Olallie watershed where only geomorphically ineffective spring-fed streams are found.

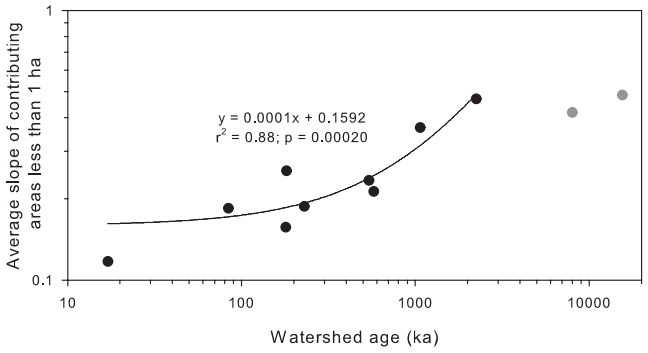

Figure 7. Average slope of DEM pixels with contributing areas less than 1 ha versus watershed age. Black circles represent the High Cascades study watersheds, and gray circles depict the Western Cascades watersheds. Linear regressions are fitted to the High Cascades data.

Landscape dissection is strongly contrasting in the two small watersheds in the south study area (NBRR, McBee). The McBee slope–area relationship has a clear inflection at $3{\cdot}6 \times 10^5$ m^2 (Figure 6h), which corresponds to the mapped channel head. In the NBRR watershed, there is little slope break at the mapped channel head (Figure 6e), possibly because most of the discharge in the stream is supplied by a spring <400 m upstream from the gaging site. McBee (1068 ka) has higher slopes than NBRR (230 ka) in unchanneled areas (Figure 7).

The three large watersheds (Lost, SFMR, MRCL) have slope–area relationships that are similar to each other, with gradually declining slopes with increasing area above ~10^4 m^2. The MRCL watershed (576 ka) has a slope break around the average contributing area of mapped channel heads (Figure 6g). In the watershed, 56% of the area is covered by <25 ka rocks and sediments and is relatively undissected. Most of the dissection in MRCL has taken place in the 25% of the watershed that is >2000 ka. In the Lost (182 ka) and SFMR (541 ka) watersheds, slopes are lowest at the highest contributing areas (Figures 6d,6f), but inflection points are somewhat masked by high slopes on steep walls of the glacial troughs. This glacial topographic signature shows up in the slope–area plots of Lost and MRCL as outlying steep slope points with contributing areas around 10^7 m^2. Such scatter in slope at high contributing areas is not found in watersheds lacking glacial troughs.

Taken together, the nine study watersheds exhibit a pattern of increasing hillslope steepness and greater slope breaks associated with channel initiation as watershed age increases. Watershed age is a strong predictor of average slope in contributing areas <1 ha (Figure 7). These results suggest a continuous process of landscape dissection that begins with the initial establishment of streams in the watershed. Comparison of >1 Ma High Cascades with the slope–area relationships of Lookout and Blue watersheds (not shown) suggests that the older High Cascades landscapes have reached the same topographic maturity as Western Cascades landscapes. Differences between the Belknap (17 ka) and Browder Creek (2242 ka) and McBee Creek (1068 ka) slope–area relationships (Figure 6) indicate that constructional morphology can be largely obliterated by hillslope, mass movement, and fluvial processes within 1 million years. In Olallie Creek (84 ka), Boulder Creek (180 ka), and NBRR (230 ka) watersheds (Figure 6), the lack of concave-up longitudinal stream profiles and slope–area scaling breaks at the channel heads suggest that fluvial erosion requires more than 200,000 years to develop its topographic signature, regardless of hydrograph characteristics and drainage density. For contributing areas $>2 \times 10^6$ m^2, all watersheds have similar slopes (<0·1), suggesting that slope is not the factor limiting fluvial erosion in the young watersheds. The heterogeneity of rock ages and conspicuous glacial erosion in the larger watersheds limits their utility in understanding the timescales of landscape dissection.

Discussion

Hydrologic and geomorphic observations portray a landscape evolving from undissected constructional volcanic morphology having bedrock groundwater drainage, to an erosional landscape having flashy hydrographs and well-developed stream networks draining steep hillslopes. This complete transformation takes ~1–2 million years on the western slopes of the Oregon Cascade Range, as evidenced by the similarities between the oldest High Cascades watersheds and Western Cascades watersheds.

In watersheds <1 Ma, well-developed stream networks having smooth, concave longitudinal profiles are not found, nor is evidence of debris flows. Rather, slope–area relationships and stream profiles seem to be controlled by a mixture of constructional form, glacial form, and transient response to base level lowering. The relative importance of each of these factors varies between watersheds, but it is clear that the landscape bears a long-lasting imprint of constructional volcanic activity. In spring-fed watersheds, landscape dissection appears to be stunted by the geomorphic ineffectiveness of spring sapping and lack of powerful peak flows, whereas in comparably-aged watersheds without springs (e.g. Boulder Creek) drainage development has progressed further. Of course, streams are curvilinear features on landscapes such as the Western Cascades and therefore occupy very small parts of their watersheds, but these well-dissected landscapes still have hillslopes with characteristic forms indicative of boundary conditions imposed by the adjacent streams. In contrast to such fluvially dominated landscapes, the weight of evidence suggests that, despite an abundance of water, most of the High Cascades landscape shows little evidence of modification by fluvial processes.

Bedrock groundwater-fed springs are the dominant mode of drainage in the youngest lavas of the west slope of the High Cascades. Radiometric dating of the spring-bearing rocks suggests that these springs can arise from rocks as old as ~700 ka, but can be absent in watersheds as young as 180 ka, because of a lack of congruence between topography and subsurface flowpaths. The absence of large springs emerging from rocks older than ~700 ka, suggests that drainage evolves away from vertical infiltration into the bedrock and towards lateral flow through the soils.

Once a basalt landscape is constructed, soil development and vegetative establishment occur within a few hundred to a few thousand years (Inbar *et al.*, 1995), but there is a 10 to 20 ka lag before surface drainage develops. This lag seems likely a result of the high permeability of young basalt. Such high permeability promotes vertical infiltration of precipitation and the formation of large groundwater systems. Indeed, bedrock groundwater-fed springs are the dominant mode of drainage in the youngest lavas of the west slope of the High Cascades. Surface drainage appears to develop opportunistically where constructional morphology concentrates groundwater discharge or where glaciers deposit till, which has a lower permeability than young basalt (10^{-9} to 10^{-15} cm^2 versus $>10^{-8}$ cm^2; Freeze and Cherry, 1979). Even in watersheds with surface drainage upslope of springs (e.g. NBRR), much of the streamflow still originates as spring-fed baseflow.

We propose that permeability reduction over time acts to reduce groundwater recharge and transmissivity of the bedrock

groundwater systems, so that drainage via shallow subsurface stormflow increases. Specifically we suggest that the switch in drainage mechanism is produced when development of low permeability soil horizons is coupled with extensive bedrock weathering. Further work on soil development, chemical weathering rates, and concomitant changes in permeability in the Oregon Cascade Range is required before our proposed mechanism explaining the switch from bedrock springs to shallow subsurface stormflow can be accepted. Nonetheless, our hypothesis is supported by work in other locations and by extrapolated estimates of chemical weathering rates, as discussed below.

Some previous work on drainage development on basalt landscapes has focused on the development of low permeability mantles on top of the basalts, from processes such as eolian deposition (Dohrenwend *et al.*, 1987; Eppes and Harrison, 1999) and *in situ* weathering and soil development (Lohse and Dietrich, 2005). Soil development resulting in low permeability, clay-rich soil layers that cause lateral subsurface and overland flow has been proposed as the cause of erosion and channel development on Hawaiian basalts (Lohse and Dietrich, 2005). Our study area is humid, densely vegetated and located upwind of the major ash-producing composite volcanoes along the Cascade crest, suggesting that dust and ash deposition rates are low relative to other volcanic regions. *In situ* soil development and till deposition are the most likely contributors to a low permeability mantle that could block groundwater recharge. Indeed, soil thickness increases rapidly with basalt age in the study area (Jefferson and Lewis, unpublished data).

The persistence of major groundwater discharge after the establishment of surface channels suggests that emplacement of a low permeability blanket on the landscape surface is insufficient to shift most flowpaths toward shallow subsurface stormflow. Instead, reduction of lava permeability must occur for bedrock groundwater to cease being the major drainage mechanism in basaltic landscapes. A likely mechanism for such permeability reduction is chemical weathering. For basalts and andesites in the western USA, weathering takes ~100,000 years to produce a sizable fraction of clay-sized particles (Colman, 1982). In Western Cascades volcanic and volcaniclastic rocks, smectite is the most abundant clay mineral, with smectite-rich soils retaining water and prone to mass wasting (Ambers, 2001). Chemical weathering rates have not been determined in the Cascade Range, but can be roughly constrained by basalt weathering rates in other places. The global runoff and temperature-based basalt weathering correlations of Dessert *et al.* (2003) yield a silicate weathering rate of ~36 t km^{-2} yr^{-1} for the study area. In the Oregon Coast Range, the chemical denudation rate calculated for a small greywacke catchment is 32 ± 10 t km^{-2} yr^{-1} (Anderson and Dietrich, 2001). These local estimates combined with studies on other basalt landscapes (Gislason *et al.*, 1996; Louvat and Allegre, 1998; Benedeti *et al.*, 2003) and the fact that basalts weather more rapidly than many other rocks (Meybeck, 1987) suggest that silicate weathering rates in the study area could be 30–50 t km^{-2} yr^{-1}. Given a bulk density of basalt of 2800 kg m^{-3}, these estimates translate to 0·011 to 0·018 mm yr^{-1}, or 11–18 m of weathering in 1 million years. Such extensive chemical weathering would have significant impacts on permeability of the basalts.

Changes in drainage density with time have been quantified for several lithologies, including glacial till (Ruhe, 1952), sedimentary rocks (Tokunaga *et al.*, 1980; Talling and Sowter, 1999), and eolian deposits on basalt lava (Wells *et al.*, 1985; Dohrenwend *et al.*, 1987). These studies span midlatitude climate zones from arid to humid, making direct comparison difficult, because of the inability to extricate lithology from climate, and we know of no other studies compiling drainage density for a chronosequence of crystalline rocks. Nonetheless, the previously published data allow calculation of drainage density doubling rates. All of the published data yield doubling times less than ~70,000 years, with the fastest drainage development occurring on glacial tills in Iowa (Ruhe, 1952), and the slowest drainage development on anticlinal conglomerates in the San Joaquin Valley, California (Talling and Sowter, 1999) In contrast, on the basalts of the High Cascades, drainage density takes ~1 million years to double from its mapped Holocene values. We suggest that the slowness of drainage development on the High Cascades landscapes is due not only to the difficulty of incising streams into bedrock, but to the lag associated with the initial establishment of channels on the landscape and to the geomorphic ineffectiveness of groundwater drainage. We hypothesize that the rate of drainage development on crystalline bedrock landscapes is, in part, a function of permeability. Further investigations of chronosequences of drainage development on other crystalline rocks would help constrain this hypothesis.

Conclusions

Hydrogeomorphic observations constrain the timescales of drainage development on the western slopes of the Oregon Cascade Range. Holocene basaltic lava flows are exclusively drained by bedrock groundwater, and there appears to be little or no drainage network development within the first 10 to 20 ka after lava emplacement. Pleistocene lava flows are drained by both groundwater and surface water, with bedrock groundwater remaining important for at least 700 ka in some watersheds, while networks fed by shallow subsurface stormflow are established in less than 200 ka in other watersheds. Large springs persist after the establishment of runoff-dominated channels upslope, so that there is a period when the two drainage mechanisms operate simultaneously. By 1 Ma, watersheds established extensive drainage networks and lacked major springs.

Observations of spring and channel morphology and hydrograph characteristics demonstrate that groundwater seepage erosion and incision by spring-fed streams are geomorphically ineffective agents of landscape change in the Oregon Cascade Range. Instead, landscape dissection seems to be driven by glacial erosion, streams fed by shallow subsurface stormflow, and debris flows on previously steepened slopes. Such stormflow produces flashy hydrographs with high peak flows capable of moving more sediment than spring-fed streams. Within 1 Ma, runoff-driven erosion completely obliterates the constructional morphology of the landscape, replacing it with steep hillslopes, extensive drainage and debris flow networks, and a clear inflection in the slope–area relationship that marks the channel initiation area.

The observed timescales for drainage development in the Oregon Cascade Range are not directly transferable to regions having different climates or geologic histories. Nonetheless, the observed sequence and evolution of drainage mechanisms may be applicable to other basalt landscapes, including places like Hawaii, Iceland, Japan, and the south-western USA. Regardless of the setting, drainage evolution on basalt landscapes likely follows the sequence of early groundwater drainage being geomorphically ineffective until replaced by a channel network with more powerful peakflows. This necessary alteration in the hydrologic flowpath partitioning may cause a lag in the landscape evolution of permeable landscapes relative to other lithologies.

Acknowledgements—This material is based upon work supported under a National Science Foundation Graduate Research Fellowship and grants from the Eugene Water and Electric Board and the Geological Society of America. We thank W. Luo for providing GIS coverages of his valley detection algorithm-derived stream network for the study area. We thank S. Majors, C. O'Connell, M. Kluber, and L. Ellenburg for assistance with field work and M.C. Rowe and M.E. Schmidt for helpful conversations. Thanks to Vic Baker and anonymous reviewer for comments on the paper and also to Paul Bishop and Mike Church for their constructive reviews of an early version of this manuscript.

References

Allison RJ, Grove JR, Higgitt DL, Kirk AJ, Rosser NJ, Warburton J. 2000. Geomorphology of the eastern Badia basalt plateau, Jordan. *Geographical Journal* **166**(4): 352–370.

Ambers RKR. 2001. Relationships between clay mineraology, hydrothermal metamorphism, and topography in a Western Cascades watershed, Oregon, USA. *Geomorphology* **38**: 47–61.

Anderson MG, Burt TP. 1978. The role of topography in controlling throughflow generation. *Earth Surface Processes and Landforms* **3**: 331–344.

Anderson SP, Dietrich WE. 2001. Chemical weathering and runoff chemistry in a steep headwater catchment. *Hydrological Processes* **15**: 1791–1815.

Baker VR. 1988. Evolution of valleys dissecting volcanoes on Mars and Earth. In *Sapping Features of the Colorado Plateau: A Comparative Planetary Geology Field Guide*, Howard AD, Kochel RC, Holt HE (eds). National Aeronautic Space Administration: Washington.

Baker VR, Gulick VC. 1987. Valley development on Hawaiian volcanoes. Technical Memorandum. 89810, National Aeronautic Space Administration: Washington.

Benedeti MF, Dia A, Riotte J, Chabaux F, Gerard M, Boulegue J, Fritz B, Chauvel C, Bulourde M, Deruelle B, Ildefonse P. 2003. Chemical weathering of basaltic lava flows undergoing extreme climatic conditions: the water geochemistry record. *Chemical Geology* **201**: 1–17.

Beven KJ, Kirkby MJ. 1978. A physically based, variable contributing area model of basin hydrology. *Hydrological Sciences Bulletin* **24**(1): 43–67.

Bishop P, Young RW, McDougall I. 1985. Stream profile change and longterm landscape evolution: early Miocene and modern rivers of the East Australian Highland Crest, Central New South Wales, Australia. *Journal of Geology* **93**: 455–474.

Bronk Ramsey C. 1995. Radiocarbon calibration and analysis of stratigraphy: the OxCal program. *Radiocarbon* **37**(2): 425–430.

Bronk Ramsey C. 2001. Development of the radiocarbon calibration program OxCal. *Radiocarbon* **43**(2A): 355–363.

Carter RW, Davidian J. 1968. General procedure for gaging streams. In *Techniques of Water-Resources Investigations of the United States Geological Survey*, Book 3 Chapter A6. US Geological Survey: Washington, DC.

Colman SM. 1982. *Chemical Weathering of Basalts and Andesites: Evidence from Weathering Rinds*. 1246, US Geological Survey: Washington.

Conrey RM, Taylor EM, Donnely-Nolan JM, Sherrod DR. 2002. North-central Oregon Cascades: exploring petrologic and tectonic intimacy in a propagating intra-arc rift. In *Field Guide to Geologic Processes in Cascadia*, Moore GW (ed). Oregon Department of Geology and Mineral Industry: Salem.

Cotton CA. 1942. *Geomorphology*. Whitcombe & Tombs Ltd: Christchurch.

Daly C, Gibson WP, Taylor GH, Johnson GL, Pasteris P. 2002. A knowledge-based approach to the statistical mapping of climate. *Climate Research* **22**: 99–113.

Davis SN. 1969. Porosity and permeability of natural materials. In *Flow Through Porous Media*, De Wiest RJM (ed). Academic Press: New York.

Dessert C, Dupre B, Gaillardet J, Francois LM, Allegre CJ. 2003. Basalt weathering laws and the impact of basalt weathering on the global carbon cycle. *Chemical Geology* **202**: 257–273.

Dohrenwend JC, Abrahams AD, Turrin BD. 1987. Drainage development on basaltic lava flows, Cima volcanic field, southeast California and Lunar Crater volcanic field, south-central Nevada. *Geological Society of America Bulletin* **99**: 405–413.

Duncan RA, Hogan LG. 1994. Radiometric dating of young MORB using the ^{40}Ar-^{39}Ar incremental heating method. *Geophysical Research Letters* **21**(18): 1927–1930.

Dunne T. 1980. Formation and controls of channel networks. *Progress in Physical Geography* **4**: 211–239.

Dunne T. 1990. Hydrology, mechanics, and geomorphic implications of erosion by subsurface flow. In *Groundwater Geomorphology: The Role of Subsurface Water in Earth-Surface Processes and Landforms*, Higgins CG, Coates DR (eds). Geological Society of America: Boulder, CO.

Dyrness CT. 1969. Hydrologic properties of soils on three small watersheds in the Western Cascades of Oregon. PNW-111, US Department of Agriculture, Forest Service Pacific Northwest Forest and Range Experimental Station, Portland, OR.

Eppes MC, Harrison JBJ. 1999. Spatial variabilty of soils developing on basalt flows in the Potrillo Volcanic Field, southern New Mexico: prelude to a chronosequence study. *Earth Surface Processes and Landforms* **24**: 1009–1024.

Flint JJ. 1974. Stream gradient as a function of order, magnitude, and discharge. *Water Resources Research* **10**: 969–973.

Freeze RA, Cherry JA. 1979. *Groundwater*. Prentice Hall: Englewood Cliffs, NJ.

Gislason SR, Arnorsson S, Armannsson H. 1996. Chemical weathering of basalt in southwest Iceland: effects of runoff, age of rocks, and vegetative/glacial cover. *American Journal of Science* **296**: 837–907.

Grant GE. 1997. A geomorphic basis for the hydrologic behavior of large river systems. In *River Quality: Dynamics and Restoration*, Laenen A, Dunnette DA (eds). Lewis Publishers: Boca Raton, FL.

Grant GE, Swanson FJ. 1995. Morphology and processes of valley floors in mountain streams, western Cascades, Oregon. In *Natural and Anthropogenic Influences in Fluvial Geomorphology*, Costa JE, Miller AJ, Potter KW and Wilcock PR (eds). American Geophysical Union: Washington, DC.

Grant GE, Swanson FJ, Wolman MG. 1990. Pattern and origin of stepped-bed morphology in high-gradient streams, Western Cascades, Oregon. *Geological Society of Americal Bulletin* **102**: 340–352.

Harr RD. 1977. Water flux in soil and subsoil on a steep forested slope. *Journal of Hydrology* **33**: 37–58.

Hattanji T, Onda Y. 2004. Coupling of runoff processes and sediment transport in mountainous watersheds underlain by different sedimentary rocks. *Hydrological Processes* **18**(4): 623–636.

Hewlett JD, Hibbert AR. 1967. Factors affecting the response of small watersheds to precipitation in humid areas. In *Forest Hydrology*, Sopper WE, Lull HW (eds). Pergammon: New York.

Horton R. 1933. The role of infiltration in the hydrologic cycle. *Transactions of the American Geophysical Union Fourteenth Annual Meeting*; 446–460.

Huang XJ, Niemann JD. 2006. Modelling the potential impacts of groundwater hydrology on long-term drainage basin evolution. *Earth Surface Processes and Landforms* **31**(14): 1802–1823.

Ijjasz-Vasquez EJ, Bras RL, Moglen GE. 1992. Sensitivity of a basin evolution model to the nature of runoff production and to initial conditions. *Water Resources Research* **28**(10): 2733–2741.

Inbar M, Risso C, Parica C. 1995. The morphological development of a young lava flow in the South Western Andes – Neuquen, Argentina. *Zoological Geomorphology* **39**(4): 479–484.

Ingebritsen SE, Sherrod DR, Mariner RH. 1992. Rates and patterns of groundwater flow in the Cascade Range volcanic arc, and the effect on subsurface temperatures. *Journal of Geophysical Research* **97**(B4): 4599–4627.

Jefferson A, Grant GE, Lewis SL. 2007. A river runs underneath it: geological control of spring and channel systems and management implications, Cascade Range, Oregon. In *Advancing the Fundamental Sciences: Proceedings of the Forest Service National Earth Sciences Conference* Furniss MJ, Clifton CF, Ronnenberg KL (eds). USDA Forest Service, PNW Research Station: Portland, OR.

Jefferson A, Grant GE, Rose TP. 2006. The influence of volcanic history on groundwater patterns on the west slope of the Oregon High Cascades. *Water Resources Research* **42**: W12411, doi:10.1029/2005WR004812.

Jefferson A, Nolin AW, Lewis SL, Tague C. 2008. Hydrogeologic controls on steamflow sensitivity to climate variation. *Hydrological Processes* **22**: 4371–4385.

Kiernan K, Wood C, Middleton G. 2003. Aquifer structure and contamination risk in lava flows: insights from Iceland and Australia. *Environmental Geology* **43**(7): 852–865.

Kilburn CRJ. 2000. Lava flows and flow fields. In *Encyclopedia of Volcanoes*, Sigurdsson H (ed). Academic Press: San Diego, CA.

Kochel RC, Baker VR. 1990. Groundwater sapping and the geomorphic development of large Hawaiian valleys. In *Groundwater Geomorphology: The Role of Subsurface Water in Earth-Surface Processes and Landforms*, Higgins CG, Coates DR (eds). Special Paper of Geological Society of America: Boulder, CO.

Kochel RC, Piper JF. 1986. Morphology of large valleys on Hawaii: evidence for groundwater sapping and comparisons with Martian valleys. *Journal of Geophysical Research* **91**(B13): E175–E192.

Koppers AAP. 2002. ArArCALC–software for $^{40}Ar/^{39}Ar$ age calculations. *Computer Geoscience* **28**: 605–619.

Lamb MP, Dietrich WE, Aciego SM, DePaolo DJ, Manga M. 2008. Formation of Box Canyon, Idaho, by megaflood: implications for seepage erosion on Earth and Mars *Science* **320**(5879): 1067–1070.

Lamb MP, Howard AD, Dietrich WE, Perron JT. 2007. Formation of amphitheater-headed valleys by waterfall erosion after large-scale slumping on Hawai'i. *Geological Society of America Bulletin* **119**(7/8): 805–822.

Lamb MP, Howard AD, Johnson J, Whipple KX, Dietrich WE, Perron JT. 2006. Can springs cut canyons into rock? *Journal of Geophysical Research* **111**: E07002, doi:10.1029/2005JE002663.

Lohse KA, Dietrich WE. 2005. Contrasting effects of soil development on hydrological properties and flow paths. *Water Resources Research* **41**: W12419, doi:10.1029/2004WR003403.

Louvat P, Allegre CJ. 1998. Riverine erosion rates on Sao Miguel volcanic island, Azores archipelago. *Chemical Geology* **148**: 177–200.

Luo W, Stepinski T. 2008. Identification of geologic contrasts from landscape dissection pattern: an application to the Cascade Range, Oregon, USA. *Geomorphology* **99**(1–4): 90–98.

Manga M. 1997. A model for discharge in spring-dominated streams and implications for the transmissivity and recharge of quaternary volcanics in the Oregon Cascades. *Water Resources Research* **33**(8): 1813–1822.

Manga M. 1999. On the timescales characterizing groundwater discharge at springs. *Journal of Hydrology* **219**: 56–69.

Meinzer OE, 1927. Large Springs in the United States. Water Supply Paper 557, United States Geological Survey, Washington.

Meybeck M. 1987. Global chemical weathering of surficial rocks estimated from river dissolved loads. *American Journal of Science* **287**(5): 401–428.

Montgomery DR, Dietrich WE. 1989. Source areas, drainage density, and channel initiation. *Water Resources Research* **25**(8): 1907–1918.

Montgomery DR, Foufoula-Georgiou E. 1993. Channel network source representation using digital elevation models. *Water Resources Research* **29**(12): 3925–3934.

Onda Y. 1992. Influence of water storage capacity in the regolith zone on hydrological characteristics, slope processes, and slope form. *Zeitschrift fur Geomorphologie* **36**(2): 165–178.

Onda Y, Tsujimura M, Fujihara J, Ito J. 2006. Runoff generation mechanisms in high-relief mountainous watersheds with different underlying geology. *Journal of Hydrology* **331**: 659–673.

Pettyjohn WA, Henning R. 1979. Preliminary estimate of groundwater recharge rates, related streamflow and water quality in Ohio. Completion Report 552, Ohio State University Water Resources Center.

Reimer PJ, Baillie MGL, Bard E, Bayliss A, Beck JW, Bertrand CJH, Blackwell PG, Buck CE, Burr GS, Cutler KB, Damon PE, Edwards RL, Fairbanks RG, Friedrich M, Guilderson TP, Hogg AG, Hughen KA, Kromer B, McCormac G, Manning S, Bronk Ramsey C, Reimer RW, Remmele S, Southon JR, Stuiver M, Talamo S, Taylor FW, van der Plicht J, Weyhenmeyer CE. 2004. IntCal04 terrestrial radiocarbon age calibration, 0–26 cal kyr BP. *Radiocarbon* **46**(3): 1029–1058.

Rose TP, Davisson ML, Criss RE. 1996. Isotope hydrology of voluminous cold springs in fractured rock from an active volcanic region, northeastern California. *Journal of Hydrology* **179**: 207–236.

Rothacher J. 1965. Streamflow from small watersheds on the western slope of the Cascade Range of Oregon. *Water Resources Research* **1**(1): 125–134.

Ruhe RV. 1952. Topographic discontinuities of the Des Moines lobe. *American Journal of Science* **250**: 46–56.

Saar MO, Manga M. 2004. Depth dependence of permeability in the Oregon Cascades inferred from hydrogeologic, thermal, seismic, and magmatic modeling constraints. *Journal of Geophysical Research* **109**(B4): B04204, 10.1029/2003JB002855.

Schmidt ME, Grunder AL. 2009. The evolution of North Sister: a volcano shaped by extension and ice in the central Oregon Cascade Arc. *Geological Society of America Bulletin* **121**(5–6): 643–662.

Schmidt ME, Grunder AL, Conrey RM, 2002. Basaltic andesite and palagonitic tuff at North Sister Volcano, Oregon High Cascades, Geological Society of America, Cordilleran Section, 98th annual meeting. Geological Society of America, Corvallis, OR.

Scott WE. 1977. Quaternary glaciation and volcanism, Metolius River area, Oregon. *Geological Society of America Bulletin* **88**: 113–124.

Scott WE, Gardner CA. 1990. Field trip guide to the central Oregon High Cascades, part I: Mount Bachelor–South Sister area. *Oregon Geology* **52**(5): 99–139.

Sherrod DR, Smith JG, 2000. Geologic Map of Upper Eocene to Holocene Volcanic and Related Rocks of the Cascade Range, Oregon. I-2569, US Geological Survey, Washington, DC.

Sherrod DR, Taylor EM, Ferns ML, Scott WE, Conrey RM, Smith GA. 2004. Geologic Map of the Bend 30- x 60-Minute Quadrangle, Central Oregon. I-2683, US Geological Survey, Washington, DC.

Sloto RA, Crouse MY. 1996. HYSEP: A computer program for streamflow hydrograph separation and analysis. Water-Reserve Investigation Report 96-4040, US Geological Survey, Washington, DC.

Soulsby C, Tetzlaff D, Rodgers P, Dunn S, Waldron S. 2006. Runoff processes, stream water residence times and controlling landscape characteristics in a mesoscale catchment: an initial evaluation. *Journal of Hydrology* **325**(1–4): 197–221.

Stearns HT, 1929. Geology and water resources of the Upper McKenzie Valley, Oregon. 597-D, US Geological Survey, Washington, DC.

Stearns HT. 1942. Hydrology of volcanic terranes. In *Hydrology*, Meinzer OE (ed). McGraw-Hill: New York.

Stock J, Dietrich WE. 2003. Valley incision by debris flows: evidence of a topographic signature. *Water Resources Research* **39**(4): 1089, doi:10.1029/2001WR001057.

Swanson FJ, Fredriksen RL. 1982. Sediment routing and budgets: implications for judging impacts of forestry practices. PNW-141, Pacific Northwest Forest and Range Experimental Station, Portland, OR.

Swanson FJ, Jones JA. 2002. Geomorphology and hydrology of the H.J. Andrews Experimental Forest, Blue River, Oregon. In *Field Guide to Geologic Processes in Cascadia*, Moore GW (ed). Oregon Department of Geology and Mineral Industries: Salem.

Tague C, Grant GE. 2004. A geological framework for interpreting the low flow regimes of Cascade streams, Willamette River Basin, Oregon. *Water Resources Research* **40**(4): W04303 10.1029/2003WR002629.

Talling PJ, Sowter MJ. 1999. Drainage density on progressively tilted surfaces with different gradients, Wheeler Ridge, California. *Earth Surface Processes and Landforms* **24**(9): 809–824.

Tarboton DG. 1997. A new method for the determination of flow directions and upslope areas in grid digital elevation models. *Water Resources Research* **33**(2): 309–319.

Tarboton DG, Bras RL, Rodriguez-Iturbe I. 1992. A physical basis for drainage density. *Geomorphology* **5**: 59–76.

Taylor GH, Hannan C. 1999. *The Climate of Oregon: From Rain Forest to Desert*. Oregon State University Press: Corvallis, OR.

Tokunaga E, Tamura T, Machida H. 1980. A morphometric study on dissection of the dated coastal terraces in South Kanto, Central Japan. *24th International Geological Congress*; 128–129.

Tucker GE, Bras RL. 1998. Hillslope processes, drainage density, and landscape morphology. *Water Resources Research* **34**(10): 2751–2764.

Tucker GE, Bras RL. 2000. A stochastic approach to modeling the role of rainfall variability in drainage basin evolution. *Water Resources Research* **36**(7): 1953–1964.

Walker GPL. 2000. Basaltic volcanoes and volcanic systems. In *Encyclopedia of Volcanoes*, Sigurdsson H (ed). Academic Press: San Diego, CA.

Welhan JA, Reed MF. 1997. Geostatistical analysis of regional hydraulic conductivity variations in the Snake River Plain aquifer, eastern Idaho. *Geological Society of America Bulletin* **109**(7): 855–868.

Wells SG, Dohrenwend JC, McFadden LD, Turrin BD, Mahrer KD. 1985. Late Cenozoic landscape evolution on lava flow surfaces of the Cima volcanic field, Mojave Desert, California. *Geological Society of America Bulletin* **96**(12): 1518–1529.

Whipple KX, Tucker GE. 1999. Dynamics of the stream-power river incision model: implications for height limits of mountain ranges, landscape response timescales, and research needs. *Journal of Geophysical Research* **104**(B8): 17661–17674.

White WB. 2002. Karst hydrology: recent developments and open questions. *Engineering Geology* **65**(2–3): 85–105.

Whiting PJ, Moog DB. 2001. The geometric, sedimentologic, and hydrologic attributes of spring-dominated channels in volcanic areas. *Geomorphology* **39**: 131–149.

Whiting PJ, Stamm J. 1995. The hydrology and form of spring-dominated channels. *Geomorphology* **12**: 223–240.

Wolman MG. 1954. A method of sampling coarse river-bed material. *American Geophysics Union Transaction* **35**(6): 951–956.

Wolman MG, Gerson R. 1978. Relative scales of time and effectiveness of climate in watershed geomorphology. *Earth Surface Processes and Landforms* **3**: 189–208.

Wolman MG, Miller JP. 1960. Magnitude and frequency of forces in geomorphic processes. *Journal of Geology* **68**: 54–74.

Wu SL, Bras RL, Barros AP. 2006. Sensitivity of channel profiles to precipitation properties in mountain ranges. *Journal of Geophysical Research-Earth Surface* **111**(F1).

